

Metamaterial-inspired multilayered structures optimized to enable wireless communications through a plasmasonic region



F SCI

Cite as: Appl. Phys. Lett. **118**, 094102 (2021); <https://doi.org/10.1063/5.0041196>

Submitted: 21 December 2020 • Accepted: 03 February 2021 • Published Online: 02 March 2021

Bruce A. Webb and  Richard W. Ziolkowski

COLLECTIONS

Paper published as part of the special topic on [Metastructures: From Physics to Application](#) This paper was selected as Featured This paper was selected as Scilight

View Online



Export Citation



CrossMark

ARTICLES YOU MAY BE INTERESTED IN

[Preventing a communication blackout in spacecraft during reentry](#)Scilight **2021**, 101104 (2021); <https://doi.org/10.1063/10.0003770>[Acceleration of radiative recombination in quasi-2D perovskite films on hyperbolic metamaterials](#)Applied Physics Letters **118**, 091104 (2021); <https://doi.org/10.1063/5.0042557>[Temporal multilayer structures for designing higher-order transfer functions using time-varying metamaterials](#)Applied Physics Letters **118**, 101901 (2021); <https://doi.org/10.1063/5.0042567>

Timing is everything.
Now it's automatic.

A new synchronous source measure system for electrical measurements of materials and devices

 [Learn more](#)

Metamaterial-inspired multilayered structures optimized to enable wireless communications through a plasmasonic region



Cite as: Appl. Phys. Lett. **118**, 094102 (2021); doi: [10.1063/5.0041196](https://doi.org/10.1063/5.0041196)
Submitted: 21 December 2020 · Accepted: 3 February 2021 ·
Published Online: 2 March 2021



View Online



Export Citation



CrossMark

Bruce A. Webb^{1,a),b)} and Richard W. Ziolkowski^{2,b),c)} 

AFFILIATIONS

¹Department of Electrical and Computer Engineering, University of Arizona, Tucson, Arizona 85721, USA

²Global Big Data Technologies Centre, University of Technology Sydney, Ultimo, NSW 2007, Australia

Note: This Paper is part of the APL Special Collection on Metastructures: From Physics to Applications.

^{a)}Also at: Radio Frequency (RF) Technologies Department, Lockheed Martin, Dallas, TX 75051.

^{b)}Authors to whom correspondence should be addressed: brucewebb@email.arizona.edu; bruce.webb@lmco.com; richard.ziolkowski@uts.edu.au; and ziolkowski@ece.arizona.edu

^{c)}Also at: Department of Electrical and Computer Engineering, University of Arizona, Tucson, AZ 85721.

ABSTRACT

Radio frequency blackout is a well-known phenomenon that happens when a plasma forms around a plasmasonic vehicle traveling through an atmosphere. This paper examines an electromagnetic metamaterial-based approach to mitigate the communication losses through the blackout plasma. A paired epsilon- and mu-negative layered meta-structure is developed that is matched to the epsilon-negative plasma, creating a low-loss passband window through it. Its ideal performance is first characterized analytically. Metamaterial inclusions are then developed to attain the required single-negative layers. Numerical simulations of the resulting realizable meta-structure verify its efficacy, confirming the analytical results and the viability of using it to achieve reasonable signal strengths through representative plasma thicknesses.

Published under license by AIP Publishing. <https://doi.org/10.1063/5.0041196>

Radio frequency (RF) blackout happens when RF transmissions used for various forms of communication by a vehicle are attenuated or reflected by the free-electron plasma it must contend with at plasmasonic speeds. The free electrons are “formed” by the dissociation from air molecules as a result of aerodynamic heating caused by the vehicle.¹ The plasma frequency varies as the square root of the plasma density and is a good indication of the amount of RF blackout expected during a planetary reentry flight. In a general sense, communication frequencies below the plasma frequency are blocked by the plasma and frequencies above the plasma frequency are transmitted with some amount of attenuation. Reentry trajectories typically generate plasma densities that result in the plasma frequency exceeding the operating frequency of the communications and telemetry systems, resulting in a communication blackout that can last anywhere from 90 s to 10 min.² Consequently, it would be very advantageous for the success of any plasmasonic mission to alleviate the blackout as much as possible. There have been many strategies considered to eliminate or reduce the RF blackout problem.² The focus in this paper is a metamaterial-based electromagnetic approach.

A material’s interaction with electromagnetic waves is determined to a large extent by its permittivity, ϵ , and permeability, μ . Further separation into positive and negative values allows categorization into four distinct types of materials: (1) materials with positive ϵ and μ , termed double-positive (DPS) media; (2) materials with negative ϵ and μ , termed double-negative (DNG) media; (3) materials with negative ϵ and positive μ , termed epsilon-negative (ENG) media; and (4) materials with negative μ and positive ϵ , termed mu-negative (MNG) media. Propagating waves can occur in DPS and DNG media; but only evanescent waves occur in a single negative (SNG) region, i.e., in ENG or MNG media.

Studies of the reentry plasma have shown that the cross section of the plasma, representing the path through which the electromagnetic wave must travel, can vary greatly in density^{3–7} as illustrated in Fig. 1. As a result, it is common to use average densities and composite parameters to characterize a reentry plasma. In this paper, the plasma is mainly viewed as a composite ENG medium as demonstrated in early reentry plasma research.⁸

Our initial considerations of the RF blackout problem were focused on the concept of combining an MNG metasurface with a

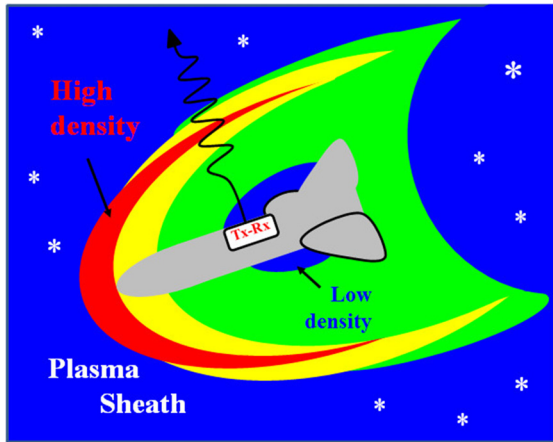


FIG. 1. Illustration of a plasma sheath surrounding a plasmasonic vehicle during reentry.

unidirectional Huygens dipole antenna to attain reasonable transmission power levels through the ENG plasma region. Herein, we emphasize the design of MNG-ENG combinations and their metamaterial realizations to achieve substantially enhanced signal transmission through longer plasma regions.

The plasma frequency is a fundamental characteristic of a plasma. It depends on its density. It is defined as $\omega_p^2 = n_e q^2 / m_e \epsilon_0$, where ω_p is the angular plasma frequency in rad/s, n_e is the electron density per unit volume, q is the charge of an electron, m_e is the mass of an electron, and ϵ_0 is the permittivity of free space.

Using the Drude model for the plasma, which is applicable in cases where a material consists of a large number of free electrons, and assuming the engineering time convention $\exp(j\omega t)$, the time harmonic form of the Drude model defines the relative permittivity of a plasma as⁹

$$\epsilon_r(\omega) = 1 - \frac{(\omega_p/\Gamma_e)^2}{1 + (\omega/\Gamma_e)^2} - j \frac{\omega_p^2/(\Gamma_e\omega)}{1 + (\omega/\Gamma_e)^2}, \quad (1)$$

where the damping rate Γ_e takes the role of the plasma collision frequency and represents the losses. Therefore, in the case of a lossless Drude material, (1) tells us that $\text{Re}[\epsilon_r(\omega)] < 0$ when $\omega < \omega_p$. Thus, a low loss plasma essentially acts as an ENG medium when the source frequency ω is smaller than the plasma frequency ω_p . This infers that the plasma acts as an ENG medium depending on its density through ω_p and Γ_e and the frequency of the field interacting with it. When the plasma acts as an ENG medium, electromagnetic waves are then evanescent in it and wireless signals are strongly attenuated as they attempt to traverse it.

To explore overcoming the attenuation associated with the ENG nature of the reentry plasma, a multi-layer structure with alternating MNG and ENG layers is introduced between the electromagnetic radiator and the plasma region. As simulated in Ref. 10, it is possible to build an equivalent DNG material with such a combination allowing wave propagation through it and ultimately the plasma. Care must be taken to establish a match between the ENG and MNG regions in order to maximize the transmission through their combination. This match is obtained by changing either the layer thicknesses or material constants.

The plasma electron density can vary substantially from near the airframe's surface to the surrounding plasma sheath to the region beyond as has been reported in a variety of works.^{4,11} An electron density of 10^{18} m^{-3} has been chosen as a reasonable intermediate value for our studies, which assumes that the antenna system is not near the nose cone of the plasmasonic vehicle where the shock-front and, hence, the most dense part of the plasma exist. When combined with the mean value of 42.5 MHz for the collision frequency, this gives $\epsilon_r = -2.06 - j0.026$ at 5.1 GHz, which we round off to $\epsilon_r = -2.0$ for simplicity. Because the evanescent wave properties of the plasma dominate its loss characteristics, this approximation value has been found to be a very reasonable choice. The 5.1 GHz operating frequency corresponds to the resonance frequency of the unidirectional Huygens dipole antenna designed for such plasma characteristics.¹²

To explore the magnitude of the propagation losses in a plasma combined with a multi-layer structure, an analytical one-dimensional (1D) multi-layer model was developed and modeled with the transfer matrix method (TMM)¹³ implemented in MATLAB. An example is shown in Fig. 2(a). Regions 1 and 4 are free space. Region 2 represents the MNG layer and region 3 represents the ENG layer, i.e., the plasma. This model is referred to as the 2-layer problem, discounting the free-space regions even though they are included in the simulation. As more MNG and ENG layers are added after the source region, the plasma region is preserved as the final region before free space, thus preserving the model as a representation of the reentry plasma problem.

However, as the plasma thickness is increased, the attenuation of a simple 2-layer solution was found to increase unavoidably.¹² It is not until adding a third layer, represented in Fig. 2(b), that the MNG and ENG material constants can be adjusted to find a solution that achieves little to no attenuation through an increasingly thick plasma as shown in Fig. 3. For the 3-layer problem, the first two layers, representing the metamaterial-based ENG and MNG media, respectively, are each held in one case to a constant 5.0 mm thickness and in the second one to an 8.0 mm thickness. The third layer that represents the plasma is varied in thickness, but its relative permittivity is held constant at the $\epsilon_r = -2.0$ value.

Adding an optimization code to the TMM simulation enabled finding suitable material parameters. However, it does result in solution lines that suffer from discontinuities (i.e., the "jumps" in the obtained values seen in Fig. 3) because an optimizer will stop when it has achieved a "close-enough" solution without thought toward any solution trends. The optimizer for the presented 3-layer case was set to simply find the minimum $|S_{11}|$ value at the selected 5.1 GHz operating frequency.

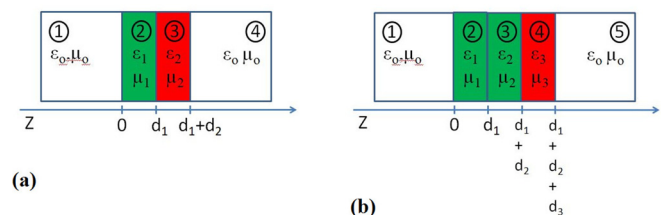


FIG. 2. TMM example problem configuration for (a) 2-layer solution and (b) 3-layer solution.

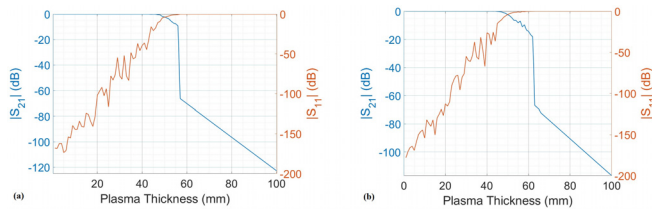


FIG. 3. S-parameters of the 3-layer TMM problem as the plasma thickness increases. (a) 5.0 mm. (b) 8.0 mm.

Both the 5.0 and 8.0 mm solutions demonstrate that essentially unity transmission and less than 10 dB attenuation can be achieved for blackout plasmas being 42–43 and 56 mm thick, respectively. Both are more than a fivefold increase over the 2-layer solution treated in Ref. 12. Although the 3-layer solutions can yield low attenuation values as the plasma thickness increases, the associated 3-dB bandwidth also significantly decreases with the optimized tuning of the layers as illustrated with the 8.0 mm layer case in Fig. 4(a). Note that the bandwidth obtained for plasma thicknesses smaller than 10 mm, the optimal case obtained in Ref. 12, is 2.0 GHz because that was the limit set for the frequency analyses, about 40% of the stipulated operating frequency. These solutions also assume that the ϵ_r and μ_r values for the first two dielectric layers are adjustable to obtain a passband solution at each plasma thickness. The dynamic range of ϵ_r in the antenna-facing ENG layer can change dramatically to match the increasing plasma thickness as demonstrated in Fig. 4(b).

However, as seen in the 8.0 mm case, the required dynamic range of the ϵ_r changes when the 8.0 mm thickness of the layers changed. By changing d_m or the refractive index n_m , the multi-layer structure can be designed to act as a bandpass filter. This response is well-known; it is what is encountered from the analysis of one-dimensional periodic structures.^{14,15}

As the thickness of layers 1 and 2 in the 3-layer model changes to accommodate different plasma thicknesses, the required dynamic ranges of the ϵ_r and μ_r change. To determine the optimal combination of the material parameters of the layers and their thickness for this multi-layer structure, the data shown in Fig. 5 were collected with the thickness of the first two layers being set to the same specific value while the plasma layer thickness remained variable. As the thickness of layers 1 and 2 in the 3-layer model change, the required dynamic ranges of ϵ_r and μ_r were found to change in quite different amounts. These ranges, as the layer thickness changes, are illustrated in Figs. 5(a) and 5(b), respectively. The values plotted represent the maximum

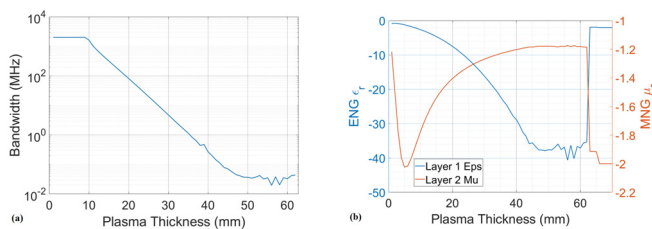


FIG. 4. Three layer solution parameter variation with increasing plasma thickness while the other layers are 8.0 mm thick. (a) Bandwidth variation and (b) required ϵ_r and μ_r values.

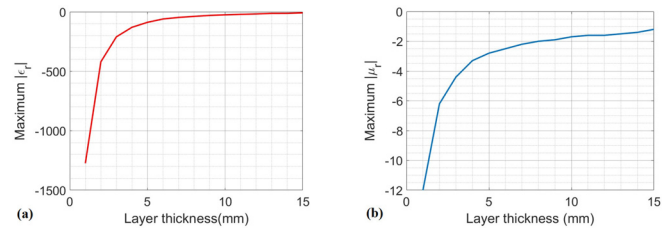


FIG. 5. The dynamic range required for the (a) ϵ_r and (b) μ_r values of the three layer solution when the equal thickness of the first two layers is adjusted.

magnitudes of the relative material parameters for any plasma thickness ≤ 100 mm.

As Fig. 5(a) indicates, a substantial material parameter variation is particularly true for the first (antenna-facing) ENG layer. Different cases indicate that ϵ_r of the first layer could need to be less than -1200 if a layer thickness of 1.0 mm was desired. However, if the layer thickness is 5.0 mm or greater, then it would only need to reach the comparatively smaller value: -100 . As the thickness increases further, ϵ_r asymptotically approaches approximately -20 . By the same token, the μ_r dynamic range starts out at a value of -12 for a 1.0 mm thickness, which is just above -3 for a 5.0 mm thickness and asymptotically approaches -1 for larger thicknesses.

The absolute values of μ_r are much smaller than those of ϵ_r by virtue of not being the first layer. For example, a much thicker first layer would be advantageous to reduce the required magnitude of ϵ_r . Then, the second layer could be thinner to maintain a given overall thickness of the meta-structure if the $|\mu_r|$ values could be larger. Consequently, it was found that the thickness of the layers, in practice, is driven by the available dynamic range of the realizable metamaterial ϵ_r and μ_r values. This does have an effect on the meta-structure design choices and will be examined further below.

Another major consideration when choosing the layer thickness is clearly the potential thickness of the plasma layer that needs to be penetrated. A value of 50 mm is a typical thickness encountered in practice. For the 3-layer solution with the $\epsilon_r = -2.0$ plasma, the maximum plasma thickness that can be matched, i.e., with attenuation less than -20 -dB, is plotted in Fig. 6. Given the fact that typical studies indicate 100-dB or more attenuation levels through the blackout plasma, this target value is a substantial increase. Notably, both the 5.0 and 8.0 mm layer thickness cases surpass this 50 mm goal. Moreover, the 8.0 mm case was found to be the optimal 3-layer solution in our parameter studies; it yielded reasonable attenuation even through a prescribed 62.0-mm-thick plasma. For these reasons, the 5.0 and 8.0 mm cases were the examples presented in Fig. 3. Further parameter studies of the multilayered structure also suggest that the thickness of each layer, d_m , for $m = 1, \dots, M$, in practice needs to be less than approximately 1/5-th of the source wavelength in air to avoid the effects of evanescent wave decay through any plasma thickness.

Another practical consideration is the bandwidth of the signal that can penetrate the plasma when the meta-structure is used. When examining Figs. 3 and 4(a) together, it is useful to note that there are three different regions associated with the attenuation characteristics of the meta-structure matched with the plasma. The first occurs when the $|S_{21}|$ is close to zero. The plasma is optimally matched and there is very good transmission through it. For both the 5.0 mm and optimal

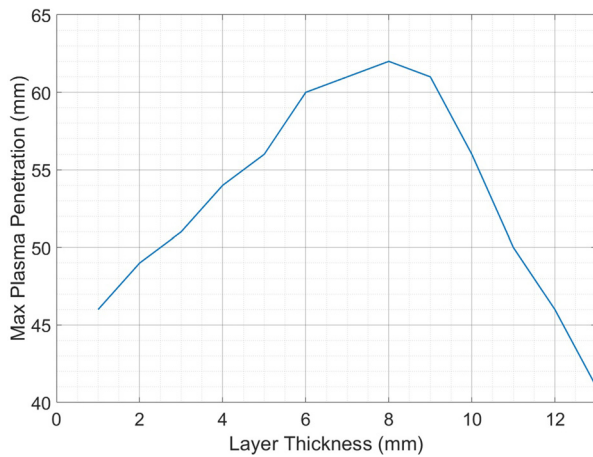


FIG. 6. Thickness of the plasma that a meta-structure with equal metamaterial ENG and MNG layer thicknesses (3-layer solution) facilitates less than a -20 -dB attenuation.

8.0 mm solutions, this region ends at a plasma thickness of about 42.0–43.0 mm. It is also found that as the plasma gets thicker, the bandwidth decreases. The second region is where the $|S_{21}|$ values begin to roll-off. This happens between plasma thicknesses of 42.0 to 56.0 mm and 43.0 to 62.0 mm in the 5.0 and 8.0 mm cases, respectively. The bandwidth at the start of this region is at or near the minimum value and does not change much throughout this region. The $|S_{21}|$ values can become lower than -20 dB at the end of this region. As the thickness of the first two layers changes, the thickness of this second region changes in size but generally starts at about the 42.0 mm plasma thickness and ends at different plasma thicknesses as demonstrated by the example cases. The start of the third region is characterized by the extreme drop in the $|S_{21}|$ value. Basically, this region has the same attenuation level as would be seen without any matching structure. In other words, the plasma thicknesses encountered in the third region have grown in size to where the RF blackout occurs despite the presence of the matching meta-structure.

We elected to use well-known ENG and MNG metamaterial inclusions to realize the meta-structure. They lend themselves to being adjustable, i.e., tunable material properties, for varying plasma conditions during the reentry trajectory. The I element (capacitively loaded strip, CLS) that was introduced for an ENG metamaterial and the ENG properties of the DNG metamaterial matched to the free-space wave impedance developed in Ref. 16 was selected for the ENG layers. Its design is illustrated in the two unit-cell simulation model shown on the left in Fig. 7. Varactors were added between the ends of the Is to provide a means to tune the relative permittivity they create. The splitting resonator (SRR) inclusions shown on the right in Fig. 7 for the same two unit-cell model were used for the MNG layers. Varactors were added across the gaps of the SRRs to provide the means to adjust the consequent μ_r values. The efficacy of such a tunable SRR-based MNG layer was demonstrated in Ref. 12.

Each inclusion was designed for one unit-cell realized on a 1.0-mm-thick sheet of the Rogers copper-clad DuroidTM 5880 substrate. If an MNG or ENG metamaterial was needed that was thicker than 1.0 mm, then repeating layers were stacked to attain the desired

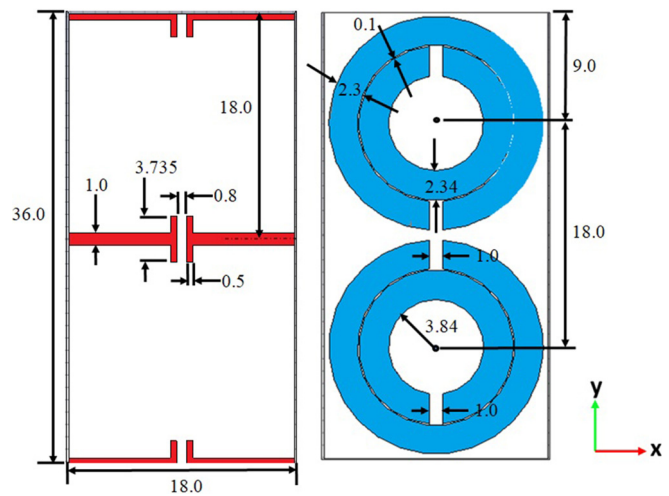


FIG. 7. I (left) and SRR (right) inclusions in the two unit-cell models of the ENG and MNG metamaterial layers and their design parameter values developed for the 3-layer solution.

thickness. To help minimize the coupling between the SRRs and the Is and, hence, to alleviate rather long design cycles, the relative positions of these two inclusions were arranged so that the Is were as far away from the center of the SRRs as possible, i.e., the SRRs were centered between the Is as shown in Fig. 7.

The simulations were performed with the frequency-domain solver within the commercial CST Microwave Studio (MWS) software environment. Several of the relevant TMM case results with the homogeneous ENG and MNG layers were first reproduced with the corresponding CST simulations. Then, the 3-layer metamaterial-based simulations were designed as the unit-cell model shown in Fig. 8. Periodic boundary conditions were applied to the four exterior side surfaces. A plane wave was normally incident on the ENG front

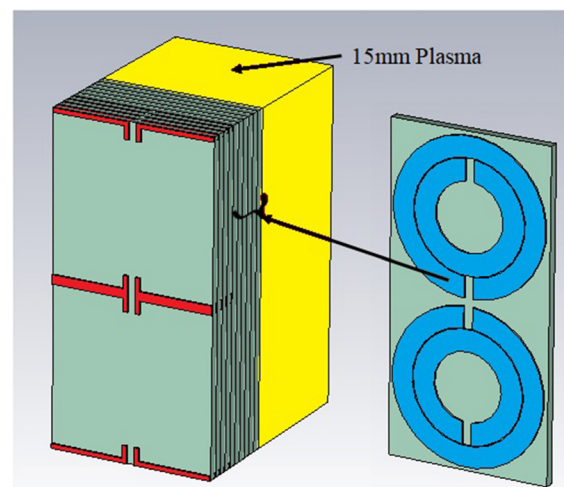


FIG. 8. CST simulation model. The ENG–MNG meta-structure is juxtaposed with the ENG plasma region.

surface of the structure. This numerical simulation model thus represented the 1D multilayered configuration corresponding to the TMM version. The materials consist of the ENG and MNG blocks and the blackout plasma as shown in Fig. 8. This transverse periodic structure corresponds to the 1D 3-layer problem depicted in Fig. 2(b).

Each metamaterial block consists of the noted eight 1.0-mm-thick layers consisting of the two unit cells with the appropriate inclusions shown in Fig. 7. The Rogers 5880 material and plasma were simulated as lossless regions with $\epsilon_r = +2.2$ and -2.0 , respectively. To save simulation time, the metal Is and SRRs were constructed as PEC traces. Moreover, because of limited computer resources, the thicknesses of the blocks and the plasma were limited to 8.0 and 15.0 mm, respectively.

The CST simulation results demonstrate the efficacy of the metamaterial designs and the resulting ENG–MNG meta-structure solution as shown in Fig. 9. The corresponding TMM results are provided for comparison. An insertion loss of only 0.12 dB was verified with the CST results. The 3-dB bandwidth through the meta-structure is 10.9 MHz, centered at 5.1 GHz. The total fractional bandwidth 0.2% is much less than the 6.3% predicted by the TMM simulation. This is expected because the composite structures formed with the SRR and I elements are resonant, narrow-band structures. Their responses limit the overall solution bandwidth. Nevertheless, an unmatched 15.0 mm plasma in comparison would normally have between 15 and 20 dB insertion loss depending on the various factors involved in its creation. The significantly enhanced transmission through this example plasma region in the presence of the meta-structure verifies its utility as an electromagnetics-based solution to the RF blackout problem.

While the evanescent wave decay in the single-negative plasma medium is the loss that is largely overcome using the developed meta-structure approach, there are also conductive losses associated with the inclusions and material losses in the meta-structure and plasma region that would be present even if the evanescent decay was totally mitigated. CST and TMM simulations have shown that the former and the latter, respectively, are indeed minor in comparison to the attenuation experienced by a wireless signal traversing the plasma region. If that signal attenuation can be significantly reduced as demonstrated herein, a more powerful wireless source can realistically overcome those remaining losses in practice.

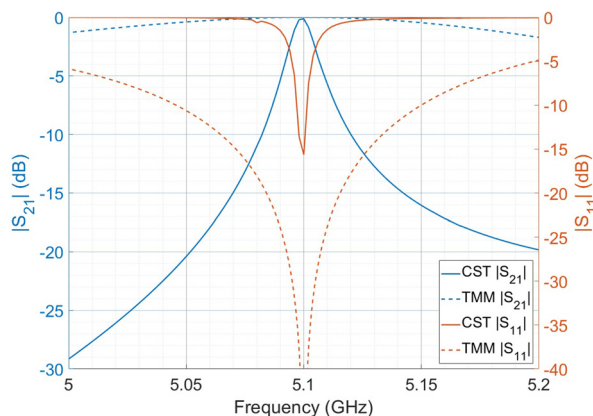


FIG. 9. CST simulated S-parameter results of the 3-layer model based on the I and SRR element realizations of the 8.0 mm ENG and MNG layers, respectively.

In a practical implementation, the metamaterial layers would have to be integrated below and on the surface of the airframe. Moreover, the meta-structure and the associated radiating system would be positioned away from the nose cone along the airframe in a region where the anticipated plasma density is low for major portions of its reentry trajectory. This configuration is depicted in Fig. 1. The 3-layer solution would have the MNG layer interfaced with the plasma in that position. For the meta-structure to survive in a hot plasma environment, the Duroid substrate would need to be replaced with a metal-clad ceramic material or something equivalent that can readily survive the high plasma temperatures it would be expected to face. The SRR and CLS-based designs can be easily refashioned to accommodate these practical concerns.

Also, note that the range of useful angles at which the associated antenna system must direct substantial power levels becomes constrained by the meta-structure and the plasma thickness. In particular, the fields that are obliquely incident on the meta-structure and that still have low reflection from it and large transmission through it and the ensuing plasma region become smaller as the plasma thickness increases. Thus, the ability to penetrate a thicker plasma comes at a cost of requiring a more directive antenna system.

As the TMM simulation results shown in Fig. 10 demonstrate, the transmission level through the plasma region varies as the angle of incidence that the field radiated by the antenna system makes with the meta-structure and as the thickness of the plasma changes. The range of these angles of incidence shrinks, for example, in the 8.0 mm-layer-thickness case from $\pm 30^\circ$ to $\pm 7^\circ$ as the plasma thickness varies from 10 to 20.0 mm. Moreover, the anisotropic nature of the metamaterial inclusions themselves will further restrict the actual allowed range of useful incidence angles. Therefore, their appropriate design would become more critical when thicker plasmas are encountered. These restrictive behaviors could be overcome by shaping the metamaterial surface to conform to the pattern radiated by the antenna system or even by using methods developed for compact antenna ranges to increase the effective distance and, hence, minimize the physical distance between it and the meta-structure to achieve the formation of a plane wave with a well-defined angle of incidence.

The design of an ENG–MNG meta-structure was examined in order to facilitate transmission through a reentry plasma. An analytical one-dimensional TMM model was implemented in MATLAB to study the effects of the materials and their thickness variations on the transmission characteristics through the plasma region. When the ENG and MNG materials were adjusted to match the plasma permittivity and thickness, the combined meta-structure produced a passband with very high transmission levels. However, as the thickness of the plasma was increased, the passband width continued to decrease in size until the maximum plasma penetration was reached at 62.0 mm and a minimum of 30 kHz bandwidth was found.

Realizable ENG and MNG metamaterial designs were developed to demonstrate the efficacy of the 3-layer solution. A CST-based unit-cell simulation of the meta-structure design achieved with I and SRR elements as the inclusions was shown to provide an insertion loss of only 0.12 dB through a 15.0-mm-thick region of the plasma. This result is significantly better than the 20 dB attenuation experienced simply trying to transmit a signal through it. However, the selected inclusions were resonant structures and did decrease the transmission level and narrow the signal bandwidth when compared to the ideal

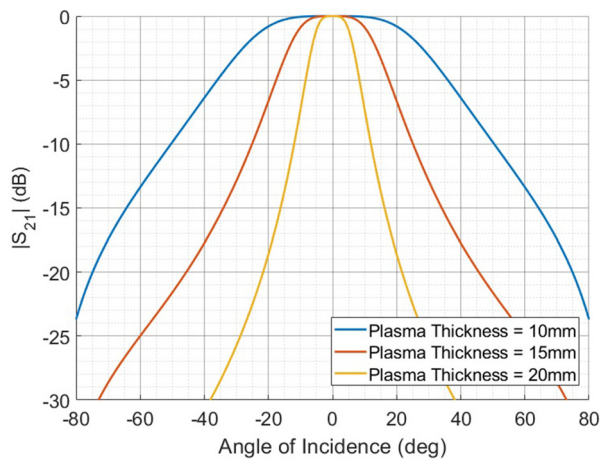


FIG. 10. TMM simulated results of the efficacy of the 3-layer model solution with the 8.0-mm-thick ENG and MNG layers as a function of the angle of incidence of the plane wave incident on the ENG layer of the ENG–MNG meta-structure.

one-dimensional TMM results. While the developed meta-structure is a demonstrated solution to the RF blackout problem faced by plasmonic vehicles, there is much research left to be done in this area and further improvements made. Nevertheless, the approach shows the potential to mitigate the majority of the problems faced when trying to communicate through the associated plasma region.

We wish to thank Professor F. Capolino and Professor M. Khajavikhan for their very kind invitation to contribute to this APL Special Topic on Metastructures.

DATA AVAILABILITY

Data sharing is not applicable to this article as no new data were created or analyzed in this study.

REFERENCES

- ¹J. D. Anderson, *Fundamentals of Aerodynamics* (McGraw-Hill Higher Education, 2001).
- ²R. A. Hartunian and G. E. Stewart, “Causes and mitigation of radio frequency (RF) blackout during reentry of reusable launch vehicles,” Report No. ATR-2007(5309)-1, The Aerospace Corporation, 2007.
- ³W. Chen, L.-X. Guo, J.-T. Li, and D. Liu, “Analysis of the electromagnetic wave scattering characteristics of time-varying plasma sheath,” *IEEE International Conference on Computational Electromagnetics (ICCEM)* (2016), pp. 40–42.
- ⁴B. W. Bai, X. P. Li, Y. M. Liu, and J. Xu, “Effects of reentry plasma sheath on mutual-coupling property of array antenna,” *Int. J. Antennas Propag.* **2015**, 542392.
- ⁵R. Savino, M. E. D’Elia, and V. Carandente, “Plasma effect on radiofrequency communications for lifting reentry vehicles,” *J. Spacecr. Rockets* **52**, 417–425 (2015).
- ⁶Y. Takahashi, R. Nakasato, and N. Oshima, “Analysis of radio frequency blackout for a blunt-body capsule in atmospheric reentry missions,” *Aerospace* **3**, 2 (2016).
- ⁷J. Ryback and R. J. Churchill, “Progress in reentry communications,” *IEEE Trans. Aerosp. Electron. Syst.* **AES-7**, 879–894 (1971).
- ⁸W. Rotman, “Plasma simulation by artificial dielectrics and parallel-plate media,” *IRE Trans. Antennas Propag.* **10**, 82–95 (1962).
- ⁹N. Engheta and R. W. Ziolkowski, “Introduction, History, and Selected Topics in Fundamental Theories of Metamaterials,” *Metamaterials: Physics and Engineering Explorations*, 1st ed. (IEEE Press, Piscataway, NJ, USA, 2006), Sec. 1.1, pp. 5–9.
- ¹⁰A. Alù and N. Engheta, “Pairing an epsilon-negative slab with a mu-negative slab: Resonance, tunneling and transparency,” *IEEE Trans. Antennas Propag.* **51**, 2558–2571 (2003).
- ¹¹X. Chen, F. F. Shen, Y. Lui, W. Ai, and X. Li, “Improved scattering-matrix method and its application to analysis of electromagnetic wave reflected by reentry plasma sheath,” *IEEE Trans. Plasma Sci.* **46**, 1755–1767 (2018).
- ¹²B. Webb and R. W. Ziolkowski, “A metamaterial-inspired approach to mitigating radio frequency blackout when a plasma forms around a reentry vehicle,” *Photonics* **7**, 88 (2020).
- ¹³R. Rumpf, “Improved formulation of scattering matrices for semi-analytical methods that is consistent with convention,” *Prog. Electromagn. Res. B* **35**, 241–261 (2011).
- ¹⁴C. A. Balanis, “Reflection and transmission of multiple interfaces,” *Advanced Engineering Electromagnetics*, 2nd ed. (Wiley and Sons, Hoboken, NJ, USA, 2012), Sec. 5.5.
- ¹⁵R. D. Meade, J. N. Winn, and J. Joannopoulos, *Photonic Crystals: Molding the Flow of Light* (Princeton University Press, Princeton, NJ, USA, 1995).
- ¹⁶R. W. Ziolkowski, “Design, fabrication, and testing of double negative metamaterials,” *IEEE Trans. Antennas Propag.* **51**, 1516–1529 (2003).